Energy Transfer from Large to Small Scales in Turbulence by Multiscale Nonlinear Strain and Vorticity Interactions

Perry L. Johnson

Phys. Rev. Lett. **124**, 104501 — Published 10 March 2020

DOI: 10.1103/PhysRevLett.124.104501

Energy Transfer from Large to Small Scales in Turbulence by Multi-scale Nonlinear Strain and Vorticity Interactions

Perry L. Johnson*
Center for Turbulence Research, Stanford University, Stanford, CA 94305, USA
(Dated: February 12, 2020)

An intrinsic feature of turbulent flows is an enhanced rate of mixing and kinetic energy dissipation due to the rapid generation of small-scale motions from large-scale excitation. The transfer of kinetic energy from large to small scales is commonly attributed to the stretching of vorticity by the strain-rate, but strain self-amplification also plays a role. Previous treatments of this connection are phenomenological or inexact, or cannot distinguish the contribution of vorticity stretching from that of strain self-amplification. In this letter, an exact relationship is derived which quantitatively establishes how intuitive multi-scale mechanisms such as vorticity stretching and strain self-amplification together actuate the inter-scale transfer of energy in turbulence. Numerical evidence verifies this result and uses it to demonstrate that the contribution of strain self-amplification to energy transfer is higher than that of vorticity stretching, but not overwhelmingly so.

Fluid turbulence is an archetypal nonlinear multi-scale phenomenon in classical physics. Encounters with turbulent flows are ubiquitous in both the natural sciences and engineering, due to the small viscosities of common fluids like air and water relative to the typical sizes and velocities in many flows. Turbulent flows are generally characterized by a continuous spectrum of energetic length and time scales, and understanding how these scales dynamically interact is a cardinal matter for turbulence modeling. The ability of turbulence to quickly produce small scale motions from large scale excitation has traditionally been characterized as a 'cascade' of energy, which has become a linchpin for the study of turbulence physics [1–6].

The stretching of vorticity by the strain-rate has been traditionally viewed as the basic mechanism by which energy is transferred from large to small scales [3, 7, 8]. In this view, coherent regions of high rotation rate (or vorticity) are preferentially subjected to extensional flow (positive strain-rate) along the axis of rotation. The conservation of angular momentum requires an increase in vorticity magnitude accompanied by a decrease in cross-section. The result is positive work done by the strain-rate on the vortex resulting in activity at smaller length scales [9]. This concept of vortex stretching has been very influential and many studies of inter-scale energy transfer in turbulence have focused on it [10–14].

A statistical (or global) connection has been established between the net amplfication of vorticity by the strain-rate and the net energy transfer to small scales using the Karman-Howarth equations [15]. While the analogy to material line stretching [7] is not perfect because vorticity does not have the same alignment behavior as passive material lines [16–18], the vorticity preferentially aligns with the strain-rate eigenvector having the second largest eigenvalue, which tends to be extensional [19–22].

The statistical connection between vorticity stretching and the energy cascade is not unique, however. An equally valid candidate mechanism is strain-rate self-amplification, i.e., the steepening of compressive strain-rates via nonlinear self-advection [23]. The positive average vorticity stretching cannot be disentangled from positive average strain self-amplification in homogeneous, or approximately locally homogeneous, flows [24]. Furthermore, truncated series expansions suggest that strain self-amplification contributes three times more than vorticity stretching to inter-scale energy transfer [25, 26].

The notion of spectral blocking in two-dimensional turbulence [27] due to the conservation of enstrophy highlights in a more precise qualitative way that vorticity stretching (which vanishes in 2D) is necessary for sustained energy transfer toward small scales. However, strain self-amplification also vanishes in 2D, and the same line of reasoning applied to the dissipation rate demonstrates that strain self-amplification is simultaneously necessary. Thus, this approach cannot distinguish between the contribution of vorticity stretching or strain self-amplification to the energy 'cascade'.

Explanations of vorticity stretching often invoke different length scales of organized strain-rate and vorticity, but (unfiltered) velocity gradients emphasize dynamics at the smallest scales [28]. Spatially filtered velocity gradients are more suited to describe behavior in the inertial range where the energy 'cascade' is a dominant feature [29]. Previous approaches using spatial filtering and/or velocity increments [25, 26, 30] have connected inertial range inter-scale energy transfer with vorticity stretching and strain self-amplification, but have essentially done so by truncating an infinite series, which leaves uncertainty regarding the role of neglected higher-order terms.

In this Letter, an exact connection is demonstrated between inter-scale energy transfer, i.e., the 'energy cascade', and spatio-temporally localized multi-scale interactions of vorticity and strain-rate in a turbulent flow. The derived relationship is verified using direct numerical simulations, and then it is further leveraged to reveal the true extent to which vorticity stretching and strain self-amplification at various scales contribute to the transfer of energy from large to small scales.

The velocity field, $\mathbf{u}(\mathbf{x},t)$, of an incompressible turbulent flow evolves according to,

$$\frac{\partial u_i}{\partial t} + u_j \frac{\partial u_i}{\partial x_j} = -\frac{1}{\rho}\frac{\partial p}{\partial x_i} + \nu \nabla^2 u_i + f_i, \tag{1}$$

where ρ is the fluid mass density, ν is the kinematic viscosity of the fluid, and $\mathbf{f}$ is any forcing applied to the fluid. The pressure field, $p(\mathbf{x},t)$, enforces the divergence-free constraint, $\nabla \cdot \mathbf{u} = 0$. The velocity gradient tensor, $A_{ij} = \partial u_i/\partial x_j$, describes the local flow topology in terms of strain-rate, $S_{ij} = \frac{1}{2}\left(A_{ij} + A_{ji}\right)$ and rotation-rate, $\Omega_{ij} = \frac{1}{2}\left(A_{ij} - A_{ji}\right)$, which can also be expressed as the vorticity vector, $\omega_i = \epsilon_{ijk}\Omega_{kj}$.

A turbulent flow with mean kinetic energy $\langle K \rangle = \frac{1}{2}\langle u_i u_i \rangle$ and mean dissipation rate $\langle \epsilon \rangle = 2\nu \langle S_{ij} S_{ij} \rangle$ is characterized by a wide range of length scales from an integral length scale, $L \sim \langle K \rangle^{3/2} \langle \epsilon \rangle^{-1}$, down to the Kolmogorov length scale, $\eta = \nu^{3/4} \langle \epsilon \rangle^{-1/4}$. The dynamic range of a turbulent flow increases as $L/\eta \sim Re_\lambda^{3/2}$, where $Re_\lambda \sim \langle K \rangle / \sqrt{\nu \langle \epsilon \rangle}$ is the Taylor-scale Reynolds number.

The features of a turbulent velocity field larger than a given scale ℓ can be isolated using a low-pass filter [31],

$$\overline{u}_i^\ell = G_\ell \star u_i, \quad \mathcal{F}\{\overline{u}_i^\ell\} = \mathcal{F}\{G_\ell\}\mathcal{F}\{u_i\}, \tag{2}$$

where $\mathcal{F}\{\cdot\}$ denotes the Fourier transform and $\star$ denotes the convolution operator. The superscript, ℓ in this case, denotes the filter width. The evolution equation for the large-scale dynamics is obtained by filtering Eq. (1),

$$\frac{\partial \overline{u}_i^\ell}{\partial t} + \overline{u}_j^\ell \frac{\partial \overline{u}_i^\ell}{\partial x_j} = -\frac{1}{\rho}\frac{\partial \overline{p}^\ell}{\partial x_i} + \nu \nabla^2 \overline{u}_i^\ell + \overline{f}_i^\ell - \frac{\partial \sigma_{ij}^\ell}{\partial x_j}, \tag{3}$$

where $\sigma_{ij}^\ell = \overline{u_i u_j}^\ell - \overline{u}_i^\ell \overline{u}_j^\ell$ represents an 'effective stress' on the large-scale velocity caused by features smaller than ℓ. The kinetic energy at scales larger than ℓ is defined as $E^\ell(\mathbf{x},t) = \frac{1}{2}\overline{\mathbf{u}}_i^\ell \overline{\mathbf{u}}_i^\ell$, and $e^\ell(\mathbf{x},t) = \frac{1}{2}\sigma_{ii}^\ell$ represents the kinetic energy at scales smaller than ℓ. The large- and small-scale energies evolve according to,

$$\frac{\partial E^\ell}{\partial t} + \frac{\partial T_i^\ell}{\partial x_i} = \overline{u}_i^\ell \overline{f}_i^\ell - \Pi^\ell - \mathcal{E}^\ell, \tag{4}$$

$$\frac{\partial e^\ell}{\partial t} + \frac{\partial t_i^\ell}{\partial x_i} = q^\ell + \Pi^\ell - \varepsilon^\ell \tag{5}$$

where T_i^ℓ and t_i^ℓ describe spatial redistribution of large- and small-scale energy, respectively (see [31] for more details). The molecular dissipation rate of large- and small-scale energy is $\mathcal{E}^\ell = 2\nu \overline{S}_{ij}^\ell \overline{S}_{ij}^\ell$ and $\varepsilon^\ell = 2\nu(\overline{S_{ij}S_{ij}}^\ell - \overline{S}_{ij}^\ell \overline{S}_{ij}^\ell)$, respectively. The work done by forcing on the small scales is $q^\ell = \overline{u_i f_i} - \overline{u}_i \overline{f}_i$. The term $\Pi^\ell = -\sigma_{ij}^\ell \overline{S}_{ij}^\ell$ appears in these two equations with opposite sign, representing energy transfer between large and small scales across scale ℓ. If energy is injected by forcing at large scales, then for a(n) (approximately) steady homogeneous flow with $\eta \ll \ell \ll L$, the energy balance becomes,

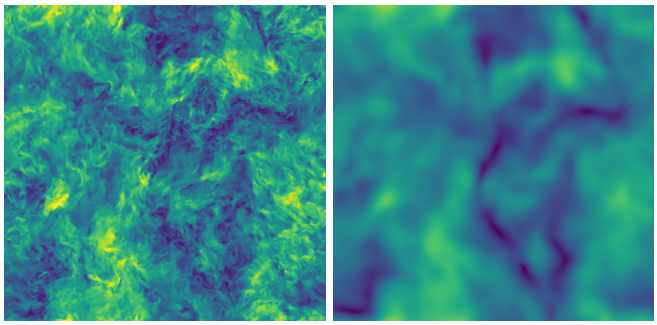

Figure 1. Unfiltered (left) and filtered (right) velocity magnitude on a slice through the 3D forced isotropic turbulence simulation at $Re_\lambda = 400$. A filter width of $\ell = 35\eta$ is used.

$$\langle u_i f_i \rangle \approx \langle \overline{u}_i^\ell \overline{f}_i^\ell \rangle \approx \langle \Pi^\ell \rangle \approx \langle \varepsilon^\ell \rangle \approx \langle \epsilon \rangle. \tag{6}$$

For the present purposes, the validity of Eq. (6) defines the inertial range of scales, where the exchange of energy across ℓ by Π^ℓ is from large to small scales in the mean in order to facilitate the dissipation of kinetic energy predominantly at small scales.

In the following, a Gaussian low-pass filter,

$$G_\ell(\mathbf{r}) = \mathcal{N} e^{-|\mathbf{r}|^2/(2\ell^2)}, \quad \mathcal{F}\{G_\ell\}(\mathbf{k}) = e^{-|\mathbf{k}|^2 \ell^2/2}, \tag{7}$$

with $\mathcal{N} = \left(2\pi\ell^2\right)^{-3/2}$, is used to derive a spatio-temporally local relationship between filtered velocity gradients and the transfer flux of energy across ℓ from large to small scales. Figure 1 shows velocity magnitude on a slice in a turbulent flow before and after the application of a Gaussian filter. It may be readily seen from Eqs. (2) and (7) that $\overline{\mathbf{u}}^\ell$ is the solution of the diffusion equation,

$$\frac{\partial \overline{u}_i^\ell}{\partial(\ell^2)} = \frac{1}{2}\nabla^2 \overline{u}_i^\ell, \quad \overline{u}_i^{\ell=0} = u_i(\mathbf{x},t), \tag{8}$$

where ℓ^2 is the time-like variable. Using the definition of σ_{ij} with Eq. (8), it is straightforward to show that the effective sub-filter scale stress may be obtained as a solution of a forced diffusion equation,

$$\frac{\partial \sigma_{ij}^\ell}{\partial(\ell^2)} = \frac{1}{2}\nabla^2 \sigma_{ij}^\ell + \overline{A}_{ik}^\ell \overline{A}_{jk}^\ell, \quad \sigma_{ij}^{\ell=0} = 0, \tag{9}$$

where $\overline{A}_{ij}^\ell$ is the filtered velocity gradient tensor.

The solution to Eq. (9), with the Gaussian kernel as the Green's function, and can be written as,

$$\sigma_{ij}^\ell = \int_0^{\ell^2} d\theta \left(\overline{\overline{A}_{ik}^{\sqrt{\theta}} \overline{A}_{jk}^{\sqrt{\theta}}}^{\sqrt{\ell^2 - \theta}} \right). \tag{10}$$

In this way, the sub-filter stress is the collective result of contributions from velocity gradient fields filtered at all scales $\sqrt{\theta}$ smaller than ℓ. The filter at $\sqrt{\ell^2-\theta}$ projects these contributions onto the larger scales.

The integrand of Eq. (10) bears some resemblance to the nonlinear model [30, 32], $\sigma_{ij}^\ell \approx \ell^2 \overline{A}_{ik}^\ell \overline{A}_{jk}^\ell$, but differs from such previous expressions in that Eq. (10) is exact rather than an approximate relation formed by truncating an infinite series. Furthermore, Eq. (10) straightforwardly decomposes into scale-local and scale-nonlocal components,

$$\sigma_{ij}^\ell = \ell^2 \overline{A}_{ik}^\ell \overline{A}_{jk}^\ell + \int_0^{\ell^2} d\theta \left(\overline{\overline{A}_{ik}^{\sqrt{\theta}} \overline{A}_{jk}^{\sqrt{\theta}}}^{\phi} - \overline{\overline{A}_{ik}^{\sqrt{\theta}}}^{\phi} \overline{\overline{A}_{jk}^{\sqrt{\theta}}}^{\phi} \right), \quad (11)$$

where $\phi = \sqrt{\ell^2-\theta}$. The first term on the right side of Eq. (11) is 'scale-local' because it only involves quantities resolved at scale ℓ. The second term involves the difference of the filtered product and the product of filtered quantities, representing the contributions of sub-filter scale velocity gradients to the stress. This is considered 'scale-nonlocal' because it contains velocity gradients at finer scales than ℓ.

Contracting Eq. (11) with the filtered strain-rate tensor forms an expression for $\Pi^\ell = -\sigma_{ij}^\ell \overline{S}_{ij}^\ell$. Then, substituting the decomposition $A_{ij} = S_{ij} + \Omega_{ij}$ leads to

$$\Pi^\ell = \Pi_{l,S}^\ell + \Pi_{l,\Omega}^\ell + \Pi_{nl,S}^\ell + \Pi_{nl,\Omega}^\ell + \Pi_{nl,c}^\ell,$$

where

$$\begin{aligned}
\Pi_{l,S}^\ell &= -\ell^2 \overline{S}_{ij}^\ell \overline{S}_{jk}^\ell \overline{S}_{ki}^\ell, \qquad \Pi_{l,\Omega}^\ell = \tfrac{1}{4}\ell^2 \overline{\omega}_i^\ell \overline{S}_{ij}^\ell \overline{\omega}_j^\ell, \\
\Pi_{nl,S}^\ell &= -\int_0^{\ell^2} d\theta \left(\overline{\overline{S}_{ik}^{\sqrt{\theta}} \overline{S}_{jk}^{\sqrt{\theta}}}^{\phi} - \overline{\overline{S}_{ik}^{\sqrt{\theta}}}^{\phi} \overline{\overline{S}_{jk}^{\sqrt{\theta}}}^{\phi} \right) \overline{S}_{ij}^\ell, \quad (12) \\
\Pi_{nl,\Omega}^\ell &= \frac{1}{4}\int_0^{\ell^2} d\theta \left(\overline{\overline{\omega}_i^{\sqrt{\theta}} \overline{\omega}_j^{\sqrt{\theta}}}^{\phi} - \overline{\overline{\omega}_i^{\sqrt{\theta}}}^{\phi} \overline{\overline{\omega}_j^{\sqrt{\theta}}}^{\phi} \right) \overline{S}_{ij}^\ell, \\
\Pi_{nl,c}^\ell &= \int_0^{\ell^2} d\theta \left(\overline{\overline{S}_{ik}^{\sqrt{\theta}} \overline{\Omega}_{jk}^{\sqrt{\theta}}}^{\phi} + \overline{\overline{\Omega}_{ik}^{\sqrt{\theta}} \overline{S}_{jk}^{\sqrt{\theta}}}^{\phi} \right) \overline{S}_{ij}^\ell.
\end{aligned}$$

The first two terms in (12) represent inter-scale energy transfer by scale-local strain-self amplification ($\Pi_{l,S}$) and scale-local vorticity stretching ($\Pi_{l,\Omega}$), respectively. By themselves, these two terms comprise the nonlinear model of Ref. [32] and are given the subscript 'l' to denote 'scale-local', expressing the fact that these terms involve only quantities filtered at scale ℓ. The remaining three terms have the subscript 'nl' for 'nonlocal', indicating that these quantities involve smaller scales than ℓ. These 'nonlocal' terms include interactions of scales only slightly smaller than ℓ, so a more intricate discussion of 'cascade' locality is included in the Supplemental Material. The third and fourth terms represent the amplification by strain at scale ℓ of sub-filter strain ($\Pi_{nl,S}$) and sub-filter vorticity ($\Pi_{nl,\Omega}$). The fifth term represents energy transfer by the resolved strain-rate tensor acting on the sub-filter correlation of strain-rate and vorticity. This energy exchange mechanism is less intuitive and has not received much attention, with the exception of [25].

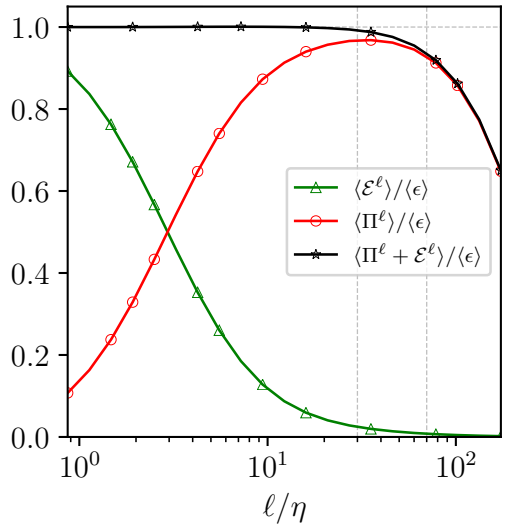

Figure 2. The resolved dissipation rate and the net inter-scale energy transfer as a function of scale using a Gaussian filter on forced isotropic turbulence at $Re_\lambda = 400$. The vertical dashed gray lines indicate $\ell = 30\eta$ and $\ell = 70\eta = 0.15L$.

The decomposition, (12)*, is exact and establishes a direct relationship, at a particular location and time in a flow, between the energy flux across scale ℓ and the multi-scale interaction of vorticity and strain.* This result enables the systematic decomposition of turbulent inter-scale energy transfer in terms of multi-scale interactions such as vorticity stretching and strain self-amplification.

To leverage this result, direct numerical simulations of steady homogeneous isotropic turbulence were performed using Eq. (1) in a triply-periodic box with forcing $\mathbf{f}$ specified such that the energy in the first two wavenumber shells remains constant. Results for a simulation with $Re_\lambda = 400$ having 1024^3 points in each direction are shown here. The range of active length scales is $L/\eta = 460$. Figure 1 illustrates the numerical simulation and filtering procedures.

The main features of energy transfer and dissipation in the simulation are shown in Figure 2 as a function of filter width, ℓ. For increasing filter width above η, the resolved dissipation rate, $\mathcal{E}^\ell$, decreases sharply and most of the viscous energy dissipation is unresolved for $\ell \gg \eta$. On the other hand, the sum of $\mathcal{E}^\ell$ and Π^ℓ is equal to the total dissipation rate provided $\ell \ll L$, which indicates the the forcing $\mathbf{f}$ is relatively inactive at these scales, see Eqs. (4) and (5). Thus, for a range of scales, $\eta \ll \ell \ll L$, the net energy transfer is equal to the total dissipation rate and Eq. (6) is approximately satisfied.

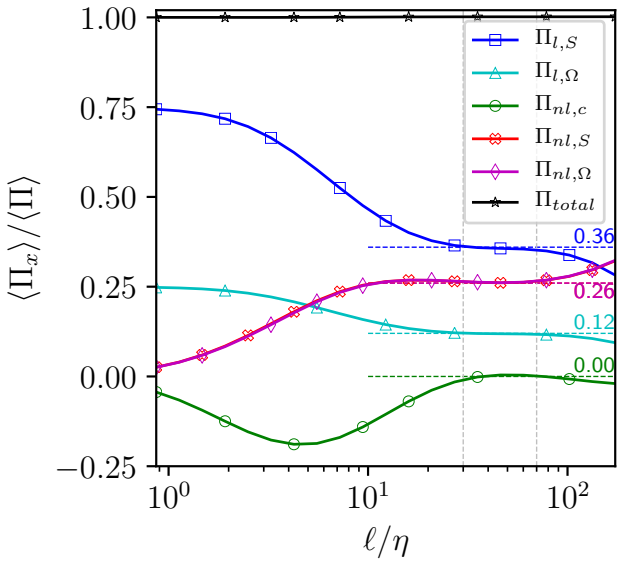

Figure 3. The fraction of net energy transfer, $\langle\Pi^\ell\rangle$, accomplished by the five mechanism from Eq. (12). The horizontal dashed lines are added manually to highlight the range of scales for which the composition of inter-scale energy transfer is approximately constant. The vertical dashed gray lines indicate $\ell = 30\eta$ and $\ell = 70\eta = 0.15L$.

Figure 3 shows the net contribution from each of the five terms in Eq. (12) as a function of filter size. The integrals are evaluated using the trapezoidal rule with a discretization over logarithmically distributed points in scale-space (θ) from $0.75\eta^2$ to ℓ^2 using roughly 15 points per decade. First, it is important to point out that the derived relation, Eq. (12), is verified by the black line marked with star symbols indicating $\langle\Pi^\ell_{total}\rangle/\langle\Pi^\ell\rangle = 1$. In other words, this confirms verifies that the ratio of the right and left sides of Eq. (12) is exactly unity for all filter widths. Next, consider separately each of the five terms on the right side of Eq. (12). For $\ell \lesssim \eta$, the nonlocal terms are small and the two local terms dominate. The Betchov relation, $\langle\Pi^\ell_{l,S}\rangle = 3\langle\Pi^\ell_{l,\Omega}\rangle$, constrains the ratio of the two local terms for any ℓ in homogeneous incompressible flows [24, 26]. As a consequence, scale-local strain self-amplification is responsible for three times more net energy transfer than scale-local vorticity stretching at any filter width.

For a range of scales approximately bounded by vertical dashed gray lines in Figures 2 and 3, the proportional contribution of each term in Eq. (12) remains fairly constant in this range of filter widths. The results show that roughly half of the net inter-scale energy transfer in the inertial range is accounted for by the local terms $\Pi^\ell_{l,S}$ and $\Pi^\ell_{l,\Omega}$. The other half is contributed by their nonlocal counterparts, $\Pi^\ell_{nl,S}$ and $\Pi^\ell_{nl,\Omega}$. In contrast to the scale-local terms, the scale-nonlocal terms indicate an even division between strain amplification and vorticity stretching on average. Due to the 'pirouette' effect [33], vorticity is known to align more efficiently with larger-scale, slower evolving strain-rates than with the strain-rate at the same scale [34, 35]. With more efficient vorticity stretching, the net inter-scale energy transfer by scale-nonlocal interactions is more evenly balanced between the two mechanisms.

To summarize, the fractional contributions of net inter-scale energy transfer from each of the five mechanisms in the inertial range can be approximately summarized as $\langle\Pi^\ell_{l,S}\rangle : \langle\Pi^\ell_{l,\Omega}\rangle : \langle\Pi^\ell_{nl,S}\rangle : \langle\Pi^\ell_{nl,\Omega}\rangle : \langle\Pi^\ell_{nl,c}\rangle \approx 3 : 1 : 2 : 2 : 0$. Including scale-local and nonlocal terms together, the ratio of contributions from strain self-amplification and vorticity stretching is roughly $\langle\Pi^\ell_S\rangle : \langle\Pi^\ell_\Omega\rangle \approx 5 : 3$. This result stands in contrast to both the traditional view which focuses only on vorticity stretching, as well as more recent views that strain self-amplification is the dominant mechanism, including the view that over-emphasizes that $\langle\Pi^\ell_{l,S}\rangle : \langle\Pi^\ell_{l,\Omega}\rangle = 3 : 1$ due to the Betchov relation [26]. The precise values found for these relative contributions are reported in Figure 3 are not emphasized because of the limited extent of inertial range provided by the present simulation. Reynolds number effects are further explored in the Supplemental Material, and future work at higher Reynolds numbers can refine these results. Dependence on filter shape is addressed in the Supplemental Material, and it is expected that the main conclusions will hold for other filter shapes [36].

In conclusion, an exact relationship between inter-scale energy transfer and multi-scale vorticity-strain interactions is introduced and verified. This development disentangles the respective impacts of vorticity stretching and strain self-amplification on the energy 'cascade'. Analysis of detailed simulations reveals that, while scale-local strain self-amplification provides three times the energy transfer as scale-local vorticity stretching, it is just as important to consider multi-scale interactions. For scale-nonlocal interactions, in fact, the net contribution by vorticity stretching and strain self-amplification is roughly equal. As a result, strain self-amplification is responsible for more net inter-scale energy transfer than vorticity stretching, but not overwhelmingly so. Both processes seem important in the rapid production of small-scale motions in turbulence.

The present view of the inter-scale energy transfer will facilitate a more detailed exploration of the energy cascade in turbulence. For instance, the efficiency of the cascade is known to be quite low [37], and the present results provide a framework for future exploration of how the cascade is driven by multi-scale velocity gradient dynamics [33, 35]. In fact, the present work suggests that it may be more advantageous to pursue shell models expressed in terms of velocity gradients [38, 39]. Also, the results shown here have focused on the net energy transfer, but this quantity fluctuates in space and time. Analysis of fluctuations and negative transfer events, as well as

investigations connecting the present work with spatially coherent structures [40, 41], may also provide a deeper mechanistic understanding of turbulent dynamics. The approach outlined here can be extended to flows with additional physics such as stratification, rotation, chemical reactions, multiple phases, and active matter.

The insights from this approach provide guidance for advancing models for large-eddy simulations, which are designed to provide accurate results despite underresolution of turbulent flows on coarse numerical grids [42, 43]. The stretching of sub-filter vorticity is an appealing basis for models [44–47], but the analysis here reveals a path for improving on such an approach.

The author would like to acknowledge support from the Advanced Simulation and Computing program of the US Department of Energy's National Nuclear Security Administration via the PSAAP-II Center at Stanford, Grant No. DE-NA0002373. The author thanks Theo Drivas, as well as Adrian Lozano-Duran and Parviz Moin for fruitful discussions on the topic. Additional thanks is due to one of the anonymous referees for pointing out the relevance of spectral blocking to this work.

* perryj@stanford.edu

[1] L. F. Richardson, *Weather Prediction by Numerical Process* (Cambridge, 1922).
[2] A. N. Kolmogorov, Dokl. Akad. Nauk SSSR **30**, 299 (1941).
[3] L. Onsager, L. Nuovo Cim. **6**, 279 (1949).
[4] U. Frisch, *Turbulence* (Cambridge, 1995).
[5] G. Falkovich, J. Phys. A-Math. Theor. **42**, 123001 (2009).
[6] L. Biferale, Annu. Rev. Fluid Mech. **35**, 441 (2003).
[7] G. I. Taylor, P. R. Soc. London A **164**, 15 (1938).
[8] D. I. Pullin and P. G. Saffman, Annu. Rev. Fluid Mech. **30**, 31 (1998).
[9] H. Tennekes and J. L. Lumley, *A First Course in Turbulence* (MIT Press, 1972).
[10] T. S. Lundgren, Phys. Fluids **25**, 2193 (1982).
[11] J. Jimenez and A. A. Wray, J. Fluid Mech. **373**, 255285 (1998).
[12] A. J. Chorin, Commun. Math. Phys. **114**, 167 (1988).
[13] A. Lozano-Duran, M. Holzner, and J. Jimenez, J. Fluid Mech. **803**, 356394 (2016).
[14] N. A. K. Doan, N. Swaminathan, P. A. Davidson, and M. Tanahashi, Phys. Rev. Fluids **3**, 084601 (2018).
[15] T. de Karman and L. Howarth, P Roy. Soc. A-Math. Phy. **164**, 192 (1938).
[16] M. Holzner, M. Guala, B. Luthi, A. Liberzon, N. Nikitin, W. Kinzelbach, and A. Tsinober, Phys. Fluids **22**, 061701 (2010).
[17] P. L. Johnson and C. Meneveau, Phys. Rev. E **93**, 033118 (2016).
[18] P. L. Johnson, S. S. Hamilton, R. Burns, and C. Meneveau, Phys. Rev. Fluids **2**, 014605 (2017).
[19] P. Vieillefosse, J. Phys.-Paris **43**, 837 (1982).
[20] P. Vieillefosse, Physica A **125**, 150 (1984).
[21] W. T. Ashurst, A. R. Kerstein, R. M. Kerr, and C. H. Gibson, Phys. Fluids **30**, 2343 (1987).
[22] B. J. Cantwell, Phys. Fluids **4**, 782 (1992).
[23] A. Tsinober, *An Informal Conceptual Introduction to Turbulence* (Springer, 2009).
[24] R. Betchov, J. Fluid Mech. **1**, 497 (1956).
[25] G. L. Eyink, J. Fluid Mech. **549**, 159 (2006).
[26] M. Carbone and A. D. Bragg, J. Fluid Mech. **883**, R2 (2020).
[27] R. Fjortoft, Tellus **5**, 225 (1953).
[28] C. Meneveau, Annu. Rev. Fluid Mech. **43**, 219 (2011).
[29] M. Danish and C. Meneveau, Phys. Rev. Fluids **3**, 044604 (2018).
[30] V. Borue and S. A. Orszag, J. Fluid Mech. **366**, 1 (1998).
[31] M. Germano, J. Fluid Mech. **238** (1992).
[32] R. A. Clark, J. H. Ferziger, and W. C. Reynolds, J. Fluid Mech. **91**, 116 (1979).
[33] H. Xu, A. Pumir, and E. Bodenschatz, Nat. Phys. **7**, 709 (2011).
[34] T. Leung, N. Swaminathan, and P. A. Davidson, J. Fluid Mech. **710**, 453481 (2012).
[35] D. Fiscaletti, G. E. Elsinga, A. Attili, F. Bisetti, and O. R. H. Buxton, Phys. Rev. Fluids **1**, 064405 (2016).
[36] See Supplemental Material [url] for more details including Reynolds number and filter shape dependencies, which includes Refs. [48–56].
[37] J. G. Ballouz and N. T. Ouellette, J. Fluid Mech. **835**, 1048 (2018).
[38] L. Biferale, L. Chevillard, C. Meneveau, and F. Toschi, Phys. Rev. Lett. **98**, 214501 (2007).
[39] P. L. Johnson and C. Meneveau, Phys. Rev. Fluids **2**, 072601(R) (2017).
[40] I. Bermejo-Moreno and D. I. Pullin, J. Fluid Mech. **603**, 101135 (2008).
[41] S. Dong, Y. Huang, X. Yuan, and A. Lozano-Duran, arXiv (2019).
[42] C. Meneveau and J. Katz, Annu. Rev. Fluid Mech. **32**, 1 (2000).
[43] P. Sagaut, *Large Eddy Simulation for Incompressible Flows* (Springer, 2006).
[44] D. I. Pullin and P. G. Saffman, Phys. Fluids **6**, 1787 (1994).
[45] A. Misra and D. I. Pullin, Phys. Fluids **9**, 2443 (1997).
[46] D. Chung and G. Matheou, J. Atmos. Sci. **71**, 1863 (2014).
[47] M. H. Silvis, R. A. Remmerswaal, and R. Verstappen, Phys. Fluids **29**, 015105 (2017).
[48] M. Germano, Phys. Fluids **29**, 1755 (1986).
[49] Vreman B, Geurts B, and Keurten H, J. Fluid Mech. **278**, p351 (1994).
[50] J. L. Lumley, Phys. Fluids **4**, 203 (1992).
[51] T. Aoyama, T. Ishihara, Y. Kaneda, M. Yokokawa, K. Itakura, and A. Uno, J. Phys. Soc. Jpn. **74**, 3202 (2005).
[52] G. L. Eyink, Physica D **207**, 91 (2005).
[53] J. A. Domaradzki and D. Carati, Phys. Fluids **19**, 085112 (2007).
[54] G. L. Eyink and H. Aluie, Phys. Fluids **21**, 115107 (2009).
[55] J. I. Cardesa, A. Vela-Martin, S. Dong, and J. Jimenez, J.nez, Phys. Fluids **27**, 111702 (2015).
[56] G. L. Eyink, "Turbulence Theory III," course notes, Johns Hopkins University (2014), http://www.ams.jhu.edu/ eyink/TurbulenceIII/notes.html.